Received: 28 April 2022 | Revised: 30 September 2022 | Accepted: 10 March 2023

DOI: 10.1111/ffe.14007

SPECIAL ISSUE ARTICLE

FFEMS Fatigue & Fracture of Engineering Materials & Structures WILEY

Formation of fine granular area in a non-defect matrix of austenitic stainless steel during very high cycle fatigue

Guocai Chai[1,2] | **Jens Bergström**[3] | **Christer Burman**[3]

[1]Engineering Materials, Linköping University, Linköping, Sweden

[2]Strategy Research, Sandvik Materials Technology, Sandviken, Sweden

[3]Karlstad University, Karlstad, Sweden

Correspondence
Guocai Chai, Strategy Research, Sandvik Materials Technology, 811 81 Sandviken, Sweden.
Email: guocai.chai@alleima.com

Abstract

A fine granular area, FGA, is a typical phenomenon observed at the very high cycle fatigue fracture crack origin with a subsurface defect in the material. The FGA has been widely investigated, and different mechanisms have been proposed. In this paper, the formation of FGA in a non-defect matrix of one austenitic steel during very high cycle fatigue was studied using a progressive stepwise load-increasing method and electron scanning microscopy/electron channeling contrast imaging (ECCI) technique. A nano rough surface area or FGA at the fatigue crack origin has been observed in the subsurface matrix without any defect. It is a new phenomenon. A mechanism was proposed using the dislocation plasticity theory. The formation of FGA in a non-defect matrix is a localized plasticity exhausting process by strain localization, grain fragmentation, stress concentration and nano crack initiation and propagation along low-angle grain boundaries.

KEYWORDS

austenitic stainless steel, dislocation, FGA, grain boundary, VHCF

Highlights

- Novel approaches were developed to study the formation of FGA in the matrix in the VHCF regime.
- FGA formed in a subsurface matrix without defect is a new observation—a material nature.
- Strain localization, dislocation sub-cell and grain fragmentation lead to nanostructure.
- Formation of FGA is due to crack initiation and propagation at low-angle grain boundary.

1 | INTRODUCTION

Very high cycle fatigue (VHCF) of metallic materials has been classified as a type of fatigue with a fatigue life beyond 10^7 loading cycles.[1] Since the earlier works,[2,3] it has become an important topic since structural integrity design and analysis of many engineering structures and components are related to fatigue in the VHCF regime in recent decades.[4–7] Great efforts have been paid to study the VHCF behavior of different metallic materials since the research of VHCF is a challenge to the traditional fatigue concept on both modes of fatigue crack initiation and fracture features.[8–11] Fatigue crack initiation in metals can shift from surface crack origin to subsurface crack origin with decreasing applied stress or increasing fatigue life from HCF to VHCF regime. Subsurface fatigue crack initiation in the VHCF regime starts mainly at subsurface defects such as inclusions, pores, and microstructure inhomogeneities,[1,4–6] but can also start in some phase or matrix that is not associated with pre-existing defects (subsurface non-defect fatigue crack origin[SNDFCO]).[4,12–14] Fatigue crack initiation at pre-existed defects has been widely investigated and reviewed.[1,4–7] For high-strength steels, fatigue crack initiation is characterized by the formation of a subsurface "fish eye,"[4] with a relatively rough surface area in the vicinity around the defect.[4,6] High-resolution scanning electron microscope (SEM) or transmission electron microscope (TEM) investigations have shown that this rough area has a fine granular microstructure and is therefore called a fine granular area (FGA).[6] Several mechanisms have been proposed to explain this phenomenon.[4,6,7,15–20] Sakai et al.[19,20] have proposed that the formation of FGA includes the following three stages: formation of a fine granular layer, nucleation and coalescence of the micro-debonding region, and finally a completed formation of an FGA. The occurrence of the dark, rough area was described as a polygonization process by the diffusion of chemical particulates during cracking. However, the paper did not provide explanations of how these three stages occurred. Hong et al.[7] have proposed numerous cyclic pressing, NCP, a model to explain the formation of FGA. The repeated cyclic loading will cause the cumulation of plastic deformation in the matrix near the inclusion, which leads to fatigue crack initiation. With further cyclic loading, the microstructure of the originated crack surfaces will be fragmented due to the crack closure and residual stress release. The original coarse grains will become nanograins due to localized intensive plastic deformation, and microstructure studies have been done to verify this model. Grad et al.[15] have proposed a model based on local plasticity in a highly stressed volume at a defect or crack tip. During cyclic loading, stress concentration around inclusion can lead to dislocation initiation and motion and a local plastic zone, which causes the formation of dislocation cells and, consequently, new finer-grain boundaries similar to the polygonization process proposed by Sakai et al.[6,20] In these models, it was proposed that small grains in metals can lead to a reduction of the threshold value of the stress intensity factor (SIF) K_{th}.[15,19] The local grain refinement leads to a sufficient decrease in the local threshold value, and a crack can initiate and propagate in the fine-grained volume.[15,19,20] Another similar model is the fragmentation of martensitic laths and the formation of dislocation cells.[21] FGA phenomena observed and studied so far are mainly correlated to inclusion/defect initiations. For VHCF origin in the matrix, there may be some weak phase,[4,12] grain boundary (GB),[12] or others not associated with pre-existing defects.[12,13] However, the mechanisms for the formation of these non-defect fatigue crack origins are still not clear.

As known, the primary cause of fatigue damage is usually intimately related to some form of cyclic slip irreversibility.[22–24] Under cyclic loading, it is now well understood that in materials having no inclusions, the crack initiates from the surface (stage I), followed by crack propagation (short and long crack, stage II).[25] In the VHCF range, surface damage becomes more or less negligibly small with a low-stress amplitude applied. Then, cracks that initiate at internal heterogeneities by stress localization or concentration can grow slowly. At the current stage, both crack initiation and growth during VHCF are still not verified physically-metallurgically. However, it was reported that cyclic strain localization has occurred as a consequence of a very high number of loading cycles in spite of the fact that the loading amplitude was below the traditional persistent slip band (PSB) threshold.[22] The high strain or stress localization can then cause fatigue damage and crack initiation.[26,27]

There are different experimental technics developed recently to study fatigue damage and crack initiation mechanisms during the VHCF process.[17,28–33] A fracture surface topographic analysis (FRASTA) method has been used to study crack initiation and propagation behavior.[17] Analytical approaches based on localized stress concentration and simulation have been used to study the large scatter of testing results.[28,29] Three-point bending[30] and stepwise load block[31] have been used to study fatigue damage. In situ damage assessment or crack initiation study using either nonlinear ultrasonic measurement[32] or synchrotron X-ray diffraction[33] are very interesting methods to study VHCF behavior.

The fatigue life of a material is commonly characterized by an S-N curve or Wöhler curve using several samples at each load level and evaluated by statistical methods. As a rapid and alternative method, the progressive stepwise load increasing test (PSLIT) to evaluate

fatigue endurance with a single sample has been proposed.[34] The cyclic loading started from a low-stress level till a certain number of cycles. Then load/stress was linearly increased until the sample failed. This method has been utilized for different materials and has shown the ability to provide reasonable material endurance limits.[35–38] Recently, this method was used to study fatigue and damage behavior in steels in the high cycle or VHCF regions.[39]In this study, the number of cycles for each load step is higher than 10^7 cycles, mostly higher than 10^8 cycles or within the VHCF regime. The results show that this method can predict the fatigue damage process, especially the damage rate in individual samples.

In the present paper, the VHCF behavior in austenitic stainless steel has been studied with the purpose of making a fundamental study on the formation of FGA in a metal matrix without defects. PSLIT is used for fatigue testing. The main assumption is that material fatigue is a local material damage process. To avoid fatigue crack initiation at the sample surface or a subsurface inclusion, high strain or stress localization in the matrix is a critical condition that can lead to fatigue damage and crack initiation.[22,26,27] Multiple crystalline materials is naturally heterogeneous due to different crystal orientations. Some crystals/grains with low Taylor factor can damage first during cyclic loading. If this damage or dislocation slipping is so small, then it may not lead to the formation of PSB, instead the formation of dislocation sub-cell or grain fragmentation, and finally the formation of crack due to plasticity exhaustion.[27] This can be obtained by localized fatigue damage in "soft grains"[40] in the matrix with PSLIT. The micro- or nanoscopic fatigue damage and crack initiation behavior are investigated using the electron channeling contrast imaging (ECCI) technique. A combination of dislocation plasticity theory and fracture mechanics has been applied, which may provide a better understanding of the formation of FGA.

2 | MATERIAL AND EXPERIMENTAL

In this investigation, one AISI 316-type austenitic stainless steel grade with high purity was used. The samples were taken in a bar material with a diameter of 15 mm, which was solution-annealed at 1050°C for 20 min and then quenched in water. Table 1 shows its chemical composition and mechanical properties. Figure 1A shows the microstructures of the material in the transversal section. The grain sizes are rather equiaxial, with a size of about 43 μm and with plenty of annealing twins.

VHCF testing was performed using an ultrasonic fatigue testing machine with a displacement-controlled mode and a frequency of 20 kHz. An hourglass geometry sample with a waist diameter of 3 mm was used (Figure 1B). A stress ratio of R = 0.1 was applied. In order to avoid excessive heating of the samples, a pressurized air-cooling was applied. To study the damage behavior, a progressive stepwise load increasing test (PSLIT) was used. Each load step was 10 MPa maintained about or more than 10^8 cycles, and then stepwise increased until the sample failed. In order to study the step length effect, the number of cycles at each step was varied from 10^8 to 10^9 cycles. Eleven samples were used. Table 2 shows the testing details of all samples with a progressive stepwise load. The last number of cycles was the cycles to failure at that stress level.

Two types of surfaces were used to study the fracture and damage behavior using an SEM. The first is the

TABLE 1 Chemical composition (wt%) and mechanical properties of the alloy used.

C	Si	Mn	Cr	Ni	N	Mo	Fe	σ_{YT} [MPa]	σ_{UT} [MPa]	A [%]
0.018	0.48	1.66	17.4	14.2	0.08	2.74	Bal.	254	605	63.4

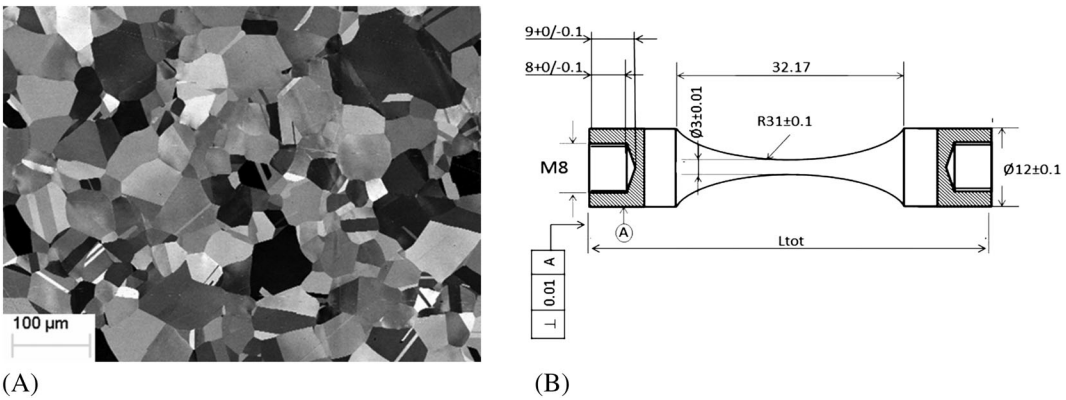

(A) (B)

FIGURE 1 (A) Microstructure of the alloy used. (B) Sample geometry used for very high cycle fatigue (VHCF) testing.

TABLE 2 Testing details with a progressive stepwise load.

Step	Stress	Spec no 1	Spec no 2	Spec no 3	Spec no 4	Spec no 5	Spec no 6	Spec no 7	Spec no 8	Spec no 9	Spec no 10	Spec no 11
	MPa	Cycles	Cycles	Cycles	Cycles	Cycles	Cycles	Cycles	Cycles	Cycles	Cycles	Cycles
1	120	1,00E+08	1,45E+08	1,19E+08	1,19E+08	1,10E+08	1,15E+08	1,34E+08	1,07E+08	1,20E+08	1,16E+08	2,65E+08
2	130	1,30E+08	1,20E+08	1,56E+08	1,51E+08	2,08E+08	2,45E+08	1,56E+08	1,62E+08	1,04E+08	1,30E+08	1,01E+08
3	140	1,37E+08	1,05E+08	2,04E+08	1,20E+08	1,67E+08	1,13E+08	1,46E+08	1,71E+08	1,80E+08	1,05E+08	1,20E+08
4	150	1,06E+08	1,19E+08	1,24E+09	1,48E+08	1,19E+09	1,19E+08	1,33E+08	1,03E+08	1,46E+09	1,06E+08	1,19E+09
5	160	1,21E+09	2,07E+08	1,87E+08	3,41E+06	1,88E+08	1,13E+06	3,05E+08	5,57E+06	1,63E+09	1,20E+09	1,23E+08
6	170	3,86E+07	1,11E+09	3,45E+09		1,62E+09				6,73E+09	5,08E+09	1,21E+08
7	180					1,60E+06				1,23E+09	1,70E+09	
8	190										3,96E+06	

original fracture surface that was used to identify the origins of fatigue crack initiation, crack initiation area or FGA and propagation behavior with striations. The other type of surface is the longitudinal section polished sample for SEM study. The method for this sample preparation has been described and discussed in the earlier works.[14,39,41] The following is a brief description of the sample preparation. A half-fatigue fractured sample was cut along the longitudinal direction through the crack initiation site. The sectioned area was then ground and mechanically polished in successive steps. For the SEM/electron channeling contrast imaging (ECCI) study, colloidal silica was applied for the final polishing stage. Thus, the sample can be used to study fatigue damage, microstructural stress concentrations (SCZ), formation of dislocation sub-cells, grain fragmentation and crack initiation/short cracks using the SEM/electron channeling contrast imaging (ECCI) technique. The microstructures at several positions from the fracture surface to the inward direction were studied.

3 | RESULTS AND DISCUSSION

3.1 | Stress versus accumulated number of cycles curves and material damage from stepwise load testing

The applied stress and accumulated number of cycles to failure, according to Table 2, are shown in Figure 2. All samples started with the same stress level of 120 MPa and a load step of 10 MPa. However, they show large scatter in both fatigue strength and total fatigue life. Sample No 9 has a total fatigue life of 1.15×10^{10} cycles, but sample No 4 has a fatigue life of 5.41×10^{8} cycles. In this paper, fatigue strength is defined as fatigue stress that has passed a given number of cycles. A VHCF strength here is defined as the stress that has passed 10^{8} cycles. Figure 2A shows that samples No 9 and No 10 have the longest total fatigue lives; the highest stress that has passed 10^{8} cycles is 180 MPa. This indicates that both samples have a fatigue strength of 180 MPa. Although a higher stress of 190 MPa was applied to sample No 10, the fatigue life is only 3.96×10^{6} cycles, less than 10^{8} cycles. Samples No 4, 6, and 8 show both the lowest fatigue lives and the lowest fatigue strength of 150 MPa. These results are contradictory to the conventional concept. Localized micro cyclic hardening is a result of this process.

Figure 2B shows the correlations between the applied stress at the last step or failure stress with the total accumulated number of cycles and a number of cycles during the last step. A longer total accumulated number of cycles may lead to a higher failure stress, as discussed

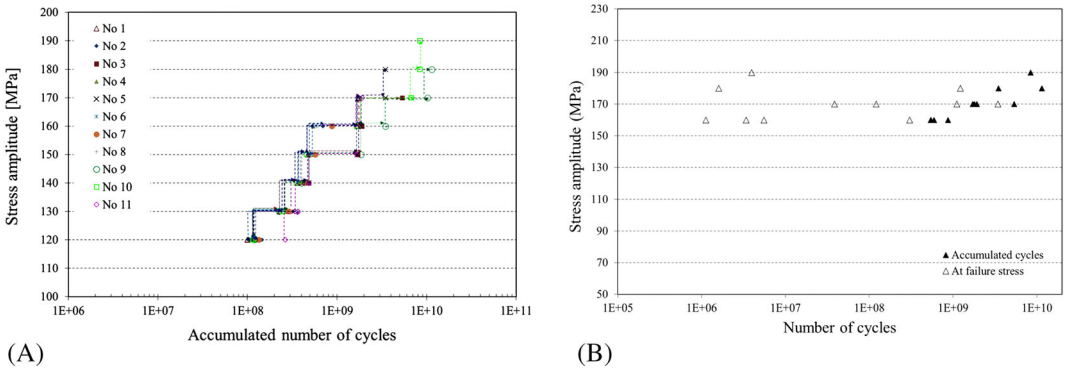

FIGURE 2 Stress and the accumulated number of cycles from the stepwise load fatigue tests. (A) With variant load steps. (B) The accumulated number of cycles to failure and cycles at failure stress of each sample. [Colour figure can be viewed at wileyonlinelibrary.com]

above. However, there is no correlation between the last applied stress and the number of fatigue life.

The above results indicate that each sample with a different number of cycles at each step can have different fatigue behavior. This may be related to the fatigue damage process during cyclic deformation at each step. The fatigue damage, D, under variable applied stress amplitude can be evaluated by Palmgren–Miner's rule with the following expression[42]:

$$D = \frac{n_1}{N_1} + \frac{n_2}{N_2} + \ldots + \frac{n_k}{N_k} = \sum_{i=1}^{k} \frac{n_i}{N_i}, \tag{1}$$

where n_i is the number of cycles accumulated at stress σ_i, and N_i is the number of cycles to failure at the i_{th} stress. When the damage D reaches a critical limit, for example, at D = 1, failure will occur.

In this paper, energy consumption, ΔU, is used to describe the fatigue damage process since the total strain energy stored in a system will be consumed by each cyclic deformation. The fatigue damage should therefore be correlated to the strain energy consumption during cyclic loading as follows.[43]

$$U = \frac{1}{2}\frac{V}{E}\sigma^2 \text{ and thus, for cyclic loading } \Delta U_i = \frac{1}{2}\frac{V}{E}N_i{\sigma_i}^2, \tag{2}$$

where U is the elastic deformation energy, ΔU_i is the energy consumed at the i_{th} load step with a maximum cyclic stress σ_i and a number of cycles N_i, E is Young's modulus, and V is the volume. The damage fraction or damage rate (D_f) of each load step is defined as follows:

$$D_f = \frac{\Delta U_i}{\sum U_i} = \frac{N_i\sigma_i^2}{\sum N_i\sigma_i^2}. \tag{3}$$

Figure 3A shows the correlation of damage fraction, $\Delta U_i/\sum \Delta U_i$, according to Equation (3) in each sample during each step versus the accumulated number of cycles. This diagram is actually related to the damage rate of each sample during the fatigue process. They show different damage evolutions. Sample No 9 shows the lowest damage levels, and samples No 4, 6, and 8 show the highest damages. These damage evolutions in Figure 3A can be strongly correlated to the total fatigue life, as shown in Figure 2B, and the fatigue strength in Table 2. They have almost the same ranks. As expected, lower damage in the sample can lead to a longer fatigue life. All curves show a similar slope, it is therefore believed that the damage mechanism in these samples during the fatigue process is similar, but the damage evolution is different, probably due to different numbers of cycles at each step that may cause different cyclic deformation responses either to damage or strengthening. The previous discussion is also confirmed by Figure 3B, which shows that the limiting failure strain energy is increasing with the number of cycles in a consistent manner. The results may also give some explanation why large scatters appear in the different samples.

This method can be used not only to study the damage and damage rate but also to qualify the material behavior during cyclic loading.

3.2 | Fatigue crack initiation and propagation

The fracture study shows that besides samples No 4, 6, and 8 with surface defect origins, all other samples have SNDFCO with a diameter of about 15–40 μm near the surface. Figure 4 shows some examples of subsurface fatigue crack initiations in the non-defect matrix. Figure 4A,B shows the fatigue crack initiation in sample No 9 after a total fatigue life of 1.15×10^{10} cycles. A fatigue crack initiation origin with an FGA near the sample surface has been observed. Different from earlier studies,[4–8,15–21] the fatigue crack initiation origin with an

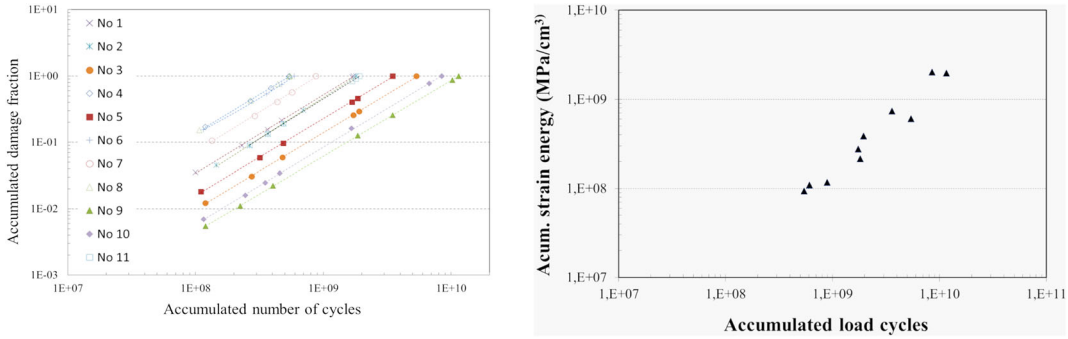

FIGURE 3 (A) Accumulated damage fraction versus the accumulated number of load cycles for each test sample. (B) Accumulated strain energy at failure for all samples tested using the progressive stepwise load increasing test (PSLIT). [Colour figure can be viewed at wileyonlinelibrary.com]

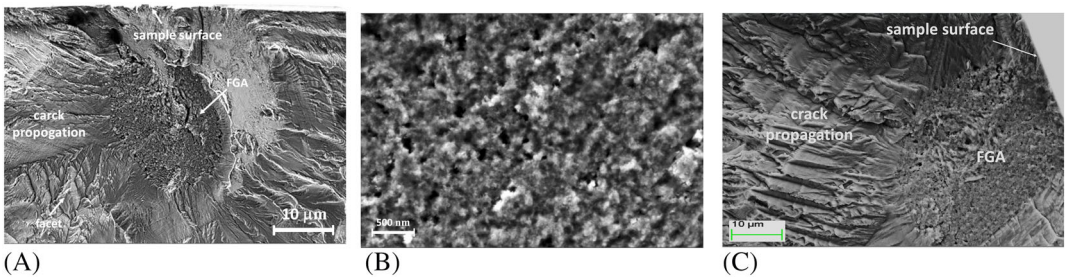

FIGURE 4 Subsurface fatigue crack initiation in the non-defect matrix. (A) Fatigue crack initiation origin with a fine granular area (FGA) in the non-defect matrix near the surface in sample No 9. (B) Enlarged FGA area in sample No 9. (C) Fatigue crack initiation origin with an FGA in the non-defect matrix near the surface in sample No 5. [Colour figure can be viewed at wileyonlinelibrary.com]

FGA observed here occurred in the matrix without any defect. This means that the fatigue damage and consequently the formation of fatigue crack initiation origin can mainly be related to the material behavior. Hence, it is of great interest to study the fundamental nature of fatigue damage in the material. This is also the first report on the formation of fatigue crack initiation origin with an FGA in this type of material. So far, we do not know where/when crack initiation or small crack propagation occurs, which will become a further investigation. The FGA in sample No 9 is similar to those observed in the subsurface inclusion crack origin.[6–8] However, this type of FGA is usually near the sample surface, as shown in Figure 4C.

In Figure 5A, a facet fracture near the FGA boundary can be observed. After a close study, very fine striations can be observed just after the FGA boundary, Figure 5B. This indicates that the crack propagation after the formation of FGA is a stage II process with multi-dislocation slip and a very low crack propagation rate. The formation of FGA is a stage I process according to the classical theory.[25] The crack propagation afterwards is similar to those of ductile materials by the formation of striations during further cyclic loading. Figure 5C shows striations formed at about 65 μm from the FGA boundary. The width of the striation is about 0.063 μm, and it still corresponds to a comparatively low crack propagation rate of 6.3×10^{-8} m/cycles.

3.3 | Formation of FGA in non-defect matrix

As known, fatigue damage in metallic material is always correlated to plastic deformation.[22–24] The FGA formations previously studied[1,4–8,15–21] are mainly related to the materials with either inclusion, multi-phase, or structure inhomogeneity. This will cause localized stress concentration at these defects and material damage during cyclic loading even with stress lower than the yield strength of the material and leads to the formation of FGA.[7,15,19,21] For a single-phase material like the austenitic stainless steel with a homogeneous structure; however, it is difficult to use the earlier theory or models to give an explanation on the formation of FGA in the material matrix without a defect.

In order to study the cyclic damage and the formation of the fine-grained structure in this homogeneous single-

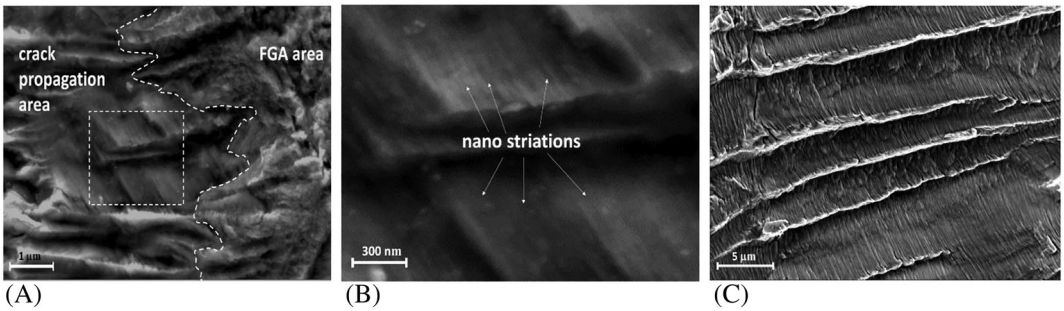

FIGURE 5 (A) Interface between fine granular area (FGA) and crack propagation in sample No 9. (B) Fatigue crack propagation near the FGA boundary (enlarged part). (C) Fatigue crack propagation at about 65 μm from the FGA boundary.

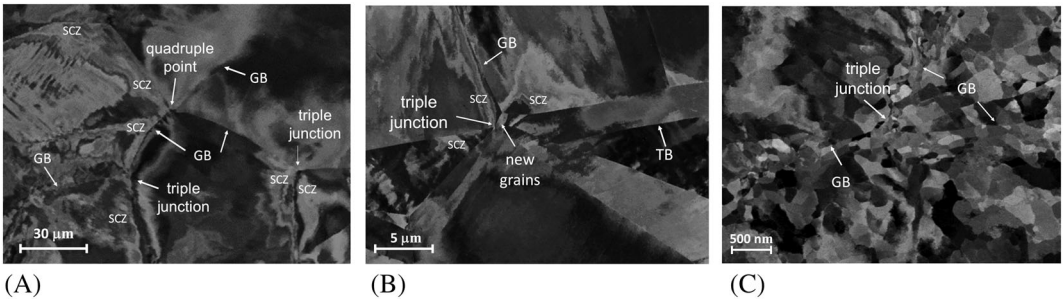

FIGURE 6 Microstructure in fatigue tested sample No 9 using SEM-ECCI. (A) Strain localization or stress concentration (SCZ) at triple or quadruple junctions, grain boundaries (GBs), and twin boundary (TB). (B) Formation of new grains at a triple junction point. (C) Grain fragmentation at a triple junction point and GBs.

phase material during the VHCF process, the microstructures of the fatigue-tested samples No 5 and No 9 from the fractured part to about 6 mm inside the polished longitudinal section samples have been studied progressively. Since an hourglass geometry sample (Figure 1B) in resonance loading was used, where the applied stress is at maximum at the sample midsection and then declines towards the sample ends, damage variations with strain or stress from the fractured part to the inside matrix can be studied. Figure 6 shows damage variations in sample No 9. In the area with less applied stress, SCZ at grain boundaries (GBs) and at GB triple and quadruple junctions can be observed (Figure 6A). With further cyclic loading/straining, new small grains can be observed at triple junctions or GBs, Figure 6B, and finally, a fine-grained structure can be observed near the fracture, Figure 6C. This indicates that strain localization during cyclic loading will cause grain fragmentation even at a low-stress amplitude.

In a polycrystalline austenitic steel, each grain has a different orientation and, consequently, different Schmid factor during loading. According to Schmid's law, a grain with a larger Schmid factor will have a higher shear stress that may lead to plastic deformation in the crystal plane and cause strain localization. Earlier studies have shown that strain localization in some grains can be more than five times higher than the average strain in the matrix in the austenitic material during VHCF, especially at low-stress amplitudes.[27,44] In certain grains, the interactions of the moving dislocations at crystal planes will form dislocation sub-cells or low-angle GBs that cause grain fragmentation.[40] This is confirmed by this work. Figure 7 shows the dislocations in the matrix and formation of dislocation sub-cells (A) and the fine low-angle GB grains (B).

Once the localized stress concentration is higher than the critical shear stress for dislocation slip, dislocations can move freely in high Schmid factor cube grains or soft grains,[40] which causes stress concentration at the GB and formation of dislocation sub-cells in the matrix during continuous deformation and crystal rotation. Grain fragmentation is a continuous process during the whole VHCF process, which causes the dislocation sub-cells to become smaller and smaller (new sub-cell in Figure 7A). On the other hand, high-strain localization can cause exhaustion of local plasticity[27] and, consequently, the formation of localized SCZ at the low-angle GBs, and it leads to crack initiation. Figure 8C shows a short crack observed in fine grains with low-angle GBs. The crack started at a triple junction point and propagated either

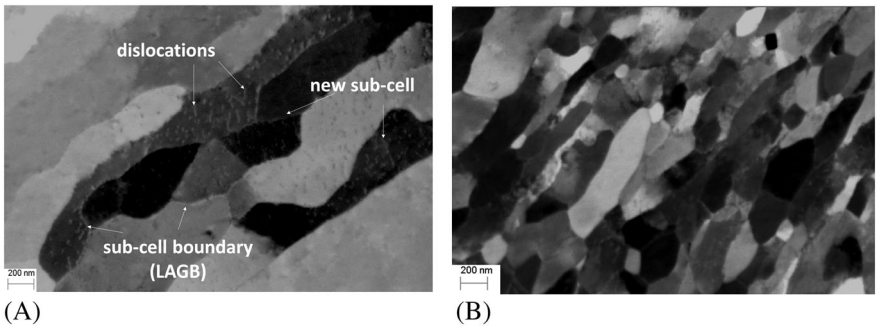

FIGURE 7 Grain fragmentation by the formation of dislocation sub-cells and nanograins with low-angle grain boundary (LAGB) in fatigue-tested sample No 5 using SEM-ECCI. (A) Formation of dislocation sub-cells and new ones. (B) Fine grains with LAGBs.

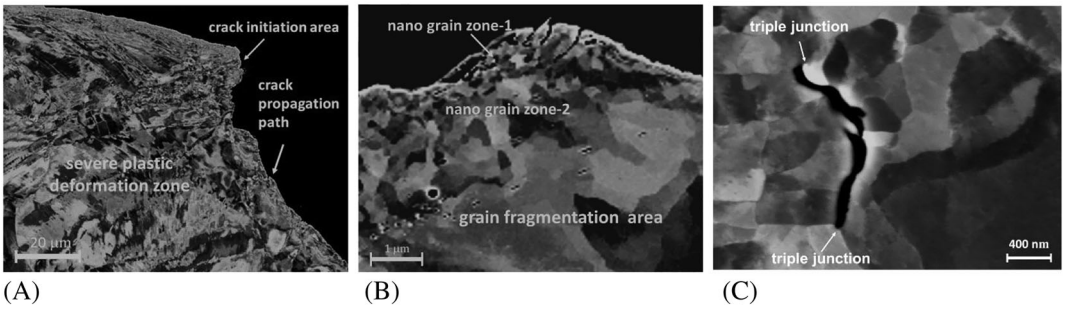

FIGURE 8 Nanograin structures formed near the fracture surface and formation of a short crack in fatigue tested sample No 9. (A) Overview of nanograin layer formed along the crack propagation path. (B) Nanograin structure layers from the crack surface towards the inside. (C) Short crack formed in nanograin zone in crack initiation area.

along the GB or across the grain in transgranular cracking and then ended at another triple junction point. The crack propagation along the GB may cause a nano-rough surface that has been observed at the FGA. This may be the crack initiation for the formation of FGA. Once this crack reaches a critical length, the crack will propagate with a normal stage II process, as discussed in references,[25,45] and an FGA has formed. It is interesting to mention that the average grain size of the material is about 43 μm, but the FGA size is between 14 to 58 μm. They have a similar size level. This may further confirm the localized damage in "soft grain" has caused the formation of FGA. Figure 8A shows the crack path from crack initiation to propagation. Fine-grained layers at the crack initiation area and a crack path near the crack initiation area were observed. This layer is rather thin, only a few micrometers, as shown in Figure 8B. This is consistent with earlier observations with focused ion beam (FIB)/TEM investigation.[20,26] Actually, there is a grain size gradient from very fine to large from the FGA to the inside of the sample. Two nanograin layers appear. Very fine nanograins can be observed near the fracture surface, and then grain size becomes progressively larger towards the inside. This further confirms that a grain fragmentation process by the formation of dislocation sub-cell or low-angle GB is a continuous process during cyclic loading/straining. The size becomes smaller near the stress/strain localization area, as shown in Figure 8C. This may also lead to a lower SIF threshold for crack propagation.[15,19]

The above results and discussion provide a proposal mechanism for the formation of FGA in a non-defect matrix of this homogeneous single-phase alloy:

1. Cyclic loading will cause stress or strain localization, especially at triple junction points and GBs.
2. Dislocation slip initiation in the localized stress concentration area causes grain fragmentation by the formation of dislocation sub-cells or low-angle GBs. The size becomes smaller with continuous cyclic loading.
3. Fatigue crack initiation starts at a low-angle GB (triple junction) due to local plasticity exhaustion.
4. Crack propagation at nanograin boundaries can cause a rough fracture surface
5. When a short crack reaches a critical size, a normal stage II crack propagation can occur, extending out of the generated FGA.

This mechanism provides a confirmation of the interesting models on the formation of FGA at a subsurface inclusion recently.[7,15,19,21,45] However, the current study provides a fundamental understanding of how material damage and crack initiation occur in a material matrix during VHCF. The formation of FGA near a subsurface

inclusion is only a special case due to the stress concentration formed near a subsurface inclusion, which may lead to a shorter VHCF life.

4 | CONCLUSIONS

Damage and formation of the FGA in a non-defect matrix of one austenitic steel submitted to VHCF were investigated, which leads to the following conclusions.

During cyclic loading within the VHCF region, strain localization will occur in the soft austenitic grains. Dislocation slipping and crystal rotation leads to the formation of dislocation sub-cells with low-angle GBs. Cyclic hardening is a result of this process.

Fatigue crack initiation will then occur at triple junction points of low-angle GBs by strain localization or stress concentration that causes localized plasticity exhaustion.

An FGA is completed once the short crack FGA propagation reaches a stress intensity threshold for further crack propagation. Crack propagation at low-angle GBs may cause a rough surface in the FGA.

The progressive stepwise load increasing test (PSLIT) is a suitable method for fundamental studies on the damage and crack initiation in pure matrix materials.

ACKNOWLEDGMENTS

This paper is published with the permission of Sandvik Materials Technology. The support of Dr. Tom Eriksson and the assistance of the ECCI study by Mr. Jerry Lindqvist are gratefully acknowledged.

DATA AVAILABILITY STATEMENT

The data that support the findings of this study are available from the corresponding author upon reasonable request.

REFERENCES

1. Stanzl SE, Tschegg E, Mayer H. Lifetime measurements for random loading in the very high cycle fatigue range. *Int J Fatigue*. 1986;8(4):195-200.
2. Atrens A, Hoffelner W, Duerig TW, Allison JE. Subsurface crack initiation in high cycle fatigue in Ti6Al4V and in a typical martensitic stainless steel. *Scripta Metall*. 1983;17(5):601-606.
3. Naito T, Ueda H, Kikuchi M. Fatigue behavior of carburized steel with internal oxides and nonmartensitic microstructure near the surface. *Metall Trans A*. 1984;5A(7):1431-1436.
4. Murakami Y. *Metal Fatigue, Effect of Small Defects and Nonmetallic Inclusion*. Elsevier Science Ltd., 0-08-044064-9; 2002.
5. Bathias C, Paris PC. In: Dekker M, ed. ISBN 0–8247–2313-9*Gigacycle Fatigue in Mechanical Practice*. CRC Press; 2004.
6. Sakai T, Harada H, Oguma N. Crack initiation mechanism of bearing steel in high cycle fatigue. In: *Fracture of Nano and Engineering Materials and Structures*. Dordrecht: Springer Netherlands; 2006:1129-1130.
7. Hong Y, Sun C. The nature and the mechanism of crack initiation and early growth for very-high-cycle fatigue of metallic materials—an overview. *Theor Appl Fract Mech*. 2017;92:331-350.
8. Sakai T. Historical review and future prospects for researches on very high cycle fatigue of metallic materials. In: *VHCF 8 digital-gesamt, Plenary 4*; 2021.
9. Sharma A, Oh MC, Ahn B. Recent advances in very high cycle fatigue behavior of metals and alloys—a review. *Metals*. 2020;10(9):1200.
10. Sippel JP, Kerscher E. Properties of the fine granular area and postulated models for its formation during very high cycle fatigue—a review. *Appl Sci*. 2020;10(23):8475.
11. Avateffazeli M, Haghshenas M. Ultrasonic fatigue of laser beam powder bed fused metals: a state-of-the-art review. *Eng Fail Anal*. 2022;134:10601, 106015.
12. Chai G. The formation of subsurface non-defect fatigue crack origins. *Int J Fatigue*. 2006;28(11):1533-1539.
13. Wang QY, Berard JY, Rathery S, Bathias C. High-cycle fatigue crack initiation and propagation behaviour of high-strength spring steel wires. *Fatigue Fract Eng Mater Struct*. 1999;22(8):673-677.
14. Tofique MW, Bergström J, Svensson K, Johansson S, Peng RL. ECCI/EBSD and TEM analysis of plastic fatigue damage accumulation responsible for fatigue crack initiation and propagation in VHCF of duplex stainless steels. *Int J Fatigue*. 2017;100:251-262.
15. Grad P, Reuscher B, Brodyanski A, Kopnarski M, Kerscher E. Mechanism of fatigue crack initiation and propagation in the very high cycle fatigue regime of high strength steels. *Scr Mater*. 2012;67(10):838-841.
16. Spriestersbach D, Kerscher E. The role of local plasticity during very high cycle fatigue crack initiation in high-strength steels. *Int J Fatigue*. 2018;111:93-100.
17. Shiozawa K, Morii Y, Nishino S, Lu L. Subsurface crack initiation and propagation mechanism in high-strength steel in a very high cycle fatigue regime. *Int J Fatigue*. 2006;28(11):1521-1532.
18. Nakamura Y, Sakai T, Hirano H, Ravi Chandran KS. Effect of alumite surface treatments on long-life fatigue behavior of a cast aluminum in rotating bending. *Int J Fatigue*. 2010;32(3):621-626.
19. Li YD, Yang ZG, Li SX, Liu YB, Chen S-M. Correlations between very high cycle fatigue properties and inclusion of GCr15 bearing steel. *Acta Metall Sin*. 2008;44:968-972.
20. Sakai T, Oguma N, Morikawa A. Microscopic and nanoscopic observations of metallurgical structures around inclusions at interior crack initiation site for a bearing steel in very high-cycle fatigue. *Fatigue Fract Eng Mater Struct*. 2015;38(11):1305-1314.
21. Zhu ML, Zhu G, Xuan FZ. On micro-defect induced cracking in very high cycle fatigue regime. *Fatigue Fract Eng Mater Struct*. 2022;45(11):1-10.
22. Mughrabi H, Höppel HW. Cyclic deformation and fatigue properties of very fine grained metals and alloys. *In J Fatigue*. 2010;32(9):1413-1427.

23. Lukáš P, Kunz L. Specific features of high-cycle and ultra-high-cycle fatigue. *Fatigue Fract Eng Mater Struct*. 2002;25(8-9):747-753.
24. Wood WA, McK Cousland S, Sargant KR. Systematic microstructural changes peculiar to fatigue deformation. *Acta Metall*. 1963;11(7):643-656.
25. Forsyth PJE. Fatigue damage and crack growth in aluminium alloys. *Acta Metall*. 1963;11(7):703-715.
26. Chai G, Forsman T, Gustavsson F, Wang C. Formation of fine grained area in martensitic steel during very high cycle fatigue. *Fatigue Fract Eng Mater Struct*. 2015;38(11):1315-1323.
27. Chai G, Zhou N, Ciurea S, Andersson M, Lin P, Ru L. Local plasticity exhaustion in a very high cycle fatigue regime. *Scripta Mater*. 2012;66(10):769-772.
28. Kolyshkin A, Zimmermann M, Kaufmann E, Christ HJ. Experimental investigation and analytical description of the damage evolution in a Ni-based superalloy beyond 10^6 loading cycles. *Int J Fatigue*. 2016;93:272-280.
29. Dönges B, Fritzen CP, Christ H. Experimental investigation and simulation of the fatigue mechanisms of a duplex stainless steel under HCF and VHCF loading conditions. *Key Eng Mater*. 2016;664:267-274.
30. Koster M, Nutz H, Freeden W, Eifler D. Measuring techniques for the very high cycle fatigue behaviour of high strength steel at ultrasonic frequencies. *Int J Mater Res*. 2012;103(1):106-112.
31. Fitzka M, Mayer H. Variable amplitude testing of 2024-T351 aluminum alloy using ultrasonic and servo-hydraulic fatigue testing equipment. *Procedia Eng*. 2015;101:169-176.
32. Kumar A, Adharapurapu RR, Jones JW, Pollock TM. In situ damage assessment in a cast magnesium alloy during very high cycle fatigue. *Scr Mater*. 2011;64(1):65-68.
33. Messager A, Junet A, Palin-Luc T, et al. In situ synchrotron ultrasonic fatigue testing device for 3D characterisation of internal crack initiation and growth. *Fatigue Fract Eng Mater Struct*. 2020;43(3):558-567.
34. Marcel PE. Fatigue test under progressive load(*). A new material testing technique. *Rev Met Paris*. 1948;45(12):481-489.
35. Thomas C, Sosa I, Setien J, Polance JC, Cimentada AI. Evaluation of the fatigue behaviour of recycled aggregate concrete. *J Clean Prod*. 2014;65:397-405.
36. Starke P, Walther F, Eifler D. 'PHYBAL' a short-time procedure for a reliable fatigue life calculation. *Adv Eng Mater*. 2012;12(4):276-282.
37. Kucharczyk P, Rizos A, Munstermann S, Bleck W. Estimation of the endurance fatigue limit for structural steel in load increasing tests at low temperature. *Fatigue Fatigue Fract Eng Mater Struct*. 2012;35(7):628-637.
38. Walther F, Eifler D. Cyclic deformation behaviour of steels and light-metal alloys. *Mater Sci Eng a Struct Mater*. 2007;468-470:259-266.
39. Chai G, Ewenz L, Persson K, Bergström J, Burman C, Zimmermann M. Fatigue behavior in metastable stainless steel during very high cycle fatigue using stepwise loading method. In: *Clinical Breast Cancer*; 2017:174-179.
40. Birosca S. The deformation behaviour of hard and soft grains in RR1000 nickel-based superalloy. *IOP Conf Ser: Mater Sci Eng*. 2015;82:012033.
41. Tofique MW, Bergström J, Svensson K. Very high cycle fatigue of cold rolled stainless steels, crack initiation and formation of the fine granular area. *Int J Fatigue*. 2017;100:238-250.
42. Miner MA. Cumulative damage in fatigue. *J Appl Mech*. 1945;12(3):159-164.
43. Hearn EJ. *Mechanics of Materials*. Butterworth-Heinemann Ltd; 1997.
44. Chai G. Analysis of microdamage in a nickel-base alloy during very high cycle fatigue. *Fatigue Fract Eng Mater Struct*. 2016;39(6):712-721.
45. Sadek M, Bergström J, Hallbäck N, Burman C, Elvira R, Escauriaza B. Fatigue strength and fracture mechanisms in the very-high-cycle-fatigue regime of automotive steels. *Steel Res Int*. 2020;91(8):2000060.

How to cite this article: Chai G, Bergström J, Burman C. Formation of fine granular area in a non-defect matrix of austenitic stainless steel during very high cycle fatigue. *Fatigue Fract Eng Mater Struct*. 2023;46(6):2364-2373. doi:10.1111/ffe.14007